CLM-P 292

United Kingdom Atomic Energy Authority
RESEARCH GROUP
Preprint

STABILITY OF LARGE AMPLITUDE RELATIVISTIC NON-LINEAR PLASMA WAVES

J JANCARIK
V N TSYTOVICH

Culham Laboratory
Abingdon Berkshire
1971

CLM - P 292

STABILITY OF LARGE AMPLITUDE RELATIVISTIC NON-LINEAR PLASMA WAVES

by

J. Jancarik

V.N. Tsytovich*

(Submitted for publication in J. Plasma Physics)

ABSTRACT

Stability properties of large amplitude, relativistic non-linear plasma waves are investigated by solving the Cauchy problem for the motion of a relativistic electron fluid with uniform stationary ion background. The development of a stationary large-amplitude relativistic wave is studied under the influence of initial perturbations of electric field and particle velocities. Stochastic initial perturbations are slightly damped with time; in the case of parametric initial perturbations a perturbation growth is followed by non-linear saturation and decay. Under some conditions particle insterstreaming can develop but it does not significantly influence the large potential wells in the wave.

*P N Lebedev Institute of Physics, Moscow, U S S R

U K A E A Research Group,
Culham Laboratory,
Abingdon,
Berks

November, 1971 (IMG)

C O N T E N T S

1. INTRODUCTION

The recent development of techniques for producing high power relativistic electron beams (see for example LINK, 1967) has revived interest in the possible interaction of such beams with plasma. One important point is that the instability is of the hydrodynamic type for a wide range of parameters so that all beam particles are resonant with the plasma wave. The phase velocity of this wave is close to the velocity of light. If the plasma density n_o is larger than the beam density n_1 and if

$$\frac{1}{\gamma^3} \ll \frac{n_1}{n_o} \ll 1 , \quad \gamma = \frac{\epsilon}{mc^2} = \frac{1}{\sqrt{1 - v^2/c^2}} , \quad \ldots (1.1)$$

where ϵ is energy of the beam particles, m and v their mass and velocity respectively, one can expect the excitation of a single mode which becomes non-linear with increasing amplitude. Although this has not yet been definitely proved, either experimentally or theoretically, this possibility increases interest in the properties of large amplitude, relativistic, non-linear waves. However, by using the results of RUBIN and TSYTOVICH (1964), one can prove that a relativistic electron ring can indeed excite such a non-linear wave when it passes through plasma (TSYTOVICH, 1970). These relativistic rings have now been produced in several laboratories (see, for example, VEKSLER et al (1967), LASSLETT et al (1969), CRISTOFILOS (1969)).

The problems associated with large amplitude non-linear relativistic plasma waves, and related to the above mentioned beam-plasma and ring-plasma interactions, can be divided into two:

(1) excitation of the waves
(2) their stability properties.

We investigate the second point, which seems to be easier to study but which also involves a large number of questions which must be answered. Let us first mention that the stationary structure of such waves has been considered by AKHIEZER et al (1951, 1955), TSYTOVICH (1962), who found that the maximum amplitude of the potential well U_{max} in the periodic structure of the wave can reach the value:

$$U_{max} \simeq 2\, m_e c^2\, \gamma_o^2 \qquad \dots (1.2)$$

where

$$\gamma_o = \frac{1}{\sqrt{1 - v_o^2/c^2}} \qquad \dots (1.3)$$

and v_o is phase velocity of the wave. If $U > U_{max}$ then a region exists in which electrons overtake the wave and the wave becomes unstable. The ions can be considered as a uniform background and are not trapped in the well (1.2) if:

$$\gamma_o < m_i/m_e \,. \qquad \dots (1.4)$$

Existence of the large well (1.2) in the case of ultra-relativistic non-linear waves allows them to be used for the collective acceleration of ions. In contrast to the case of the acceleration of a collective electron ring (VEKSLER et al, 1967), the well is not produced by the accelerated particles but by oscillating plasma particles. The problem of stability of the subsequent bunches arising from the non-linear wave is also of interest. The stability of non-relativistic plasma waves has been investigated by ROWLANDS (1969) but the relativistic case has not been considered. It is probable that relativistic plasma waves have different stability properties due to their large amplitude. Indeed, the instability must develop to a high energy level to be able to destroy such a wave, since the energy of the particles in the wave motion is high. Therefore, large perturbations and a non-linear treatment must be used to study this problem.

We first give a solution of the Cauchy problem for an arbitrary motion of a relativistic electron fluid with a uniform, constant ion background which compensates the mean charge density of the electrons (Section 2). We next present the results of a numerical solution for the structure of a stationary, large amplitude, relativistic non-linear wave (Section 4). These show how the potential wells produced by the electrons in such a wave depend on its amplitude In the following, Sections 5,7, the results of the time development of the wave in the presence of perturbations is investigated. The perturbations are assumed to be both of a stochastic and a regular nature. The cases of perturbations, both short and long, compared to the wave-length of the stationary wave are considered. The problems associated with the possible appearance of interstreaming of particles leading to instability are investigated in section 5.

2. SOLUTION OF THE CAUCHY PROBLEM*

It is convenient to write the equation describing the arbitrary one-dimensional motion of a relativistic electron fluid in the co-ordinate system in which the ions move with velocity v_0 close to c. We denote

$$\gamma_0 = \frac{1}{\sqrt{1 - v_0^2}} \; . \qquad \ldots (2.1)$$

From here on all quantities are normalized so that $c = 1$. The velocity v_0 is the phase velocity of the stationary non-linear wave. Thus, in this co-ordinate system the profile of the wave does not change in time (in the absence of perturbations). Instead of the velocity v of the relativistic electrons we use the value :

$$\gamma = \frac{1}{\sqrt{1 - v^2}} \; . \qquad \ldots (2.2)$$

The equation for the one-dimensional motion of the relativistic electron fluid has the form (see TSYTOVICH, 1961)

$$\frac{\partial \gamma}{\partial \tilde{\zeta}} + \frac{\gamma}{\sqrt{\gamma^2 - 1}} \; \frac{\partial \gamma}{\partial \tilde{\tau}} = - \tilde{\varepsilon} \qquad \ldots (2.3)$$

---

*This calculation was partially done by S.B. Rubin (J.J.P.R. Dubna) and one of the present authors (V. Tsytovich).

where

$$\tilde{\zeta} = z \frac{\omega_{pe}}{c} \qquad \ldots (2.4)$$

is the dimensionless co-ordinate , (z is the space co-ordinate of the fluid motion) and

$$\tilde{\tau} = t\, \omega_{pe} \qquad \ldots (2.5)$$

where $\tilde{\tau}$ is time in dimensionless units. Here ω_{pe} is the plasma frequency

$$\omega_{pe}^2 = \frac{4\pi n_o e^2}{m_e} \qquad \ldots (2.6)$$

where n_o is the number density of the uniformly distributed ions. The left hand side of (2.3) can easily be shown to be equal to $1/m(dp/d\tilde{\tau} + v\; dp/d\tilde{\zeta})$ where $p = mv/\sqrt{1-v^2}$. The right hand side of (2.3) is the dimensionless longitudinal electric field in the plasma

$$\tilde{\varepsilon} = \frac{E}{e\,\omega_{pe}} r_o \quad ; \quad r_o = \frac{e^2}{mc^2} . \qquad \ldots (2.7)$$

In this notation Poisson's equation becomes:

$$\frac{\partial \tilde{\varepsilon}}{\partial \tilde{\zeta}} = \gamma_o - \frac{n}{n_o}\gamma \qquad \ldots (2.8)$$

where γ_o represents the uniform charge density of the ion background and $(n/n_o)\gamma$ the charge density of the electrons (n is the electron density). The Maxwell equation $\partial E/\partial t + 4\pi j/c = \text{curl}\, H = 0$ gives

$$\frac{\partial \tilde{\varepsilon}}{\partial \tilde{\tau}} = -\sqrt{\gamma_o^2 - 1} + \frac{n}{n_o}\sqrt{\gamma^2 - 1} . \qquad \ldots (2.9)$$

From equations (2.8) and (2.9) one can easily find the density n and the equation for $\tilde{\varepsilon}$

$$\frac{\partial \tilde{\varepsilon}}{\partial \tilde{\zeta}} + \frac{\gamma}{\sqrt{\gamma^2 - 1}} \frac{\partial \tilde{\varepsilon}}{\partial \tilde{\tau}} = \gamma_0 - \frac{\gamma}{\sqrt{\gamma^2 - 1}} \sqrt{\gamma_0^2 - 1} \ . \qquad \ldots \ (2.10)$$

From equations (2.3) and (2.10), two coupled equations for the two variables γ and ε can be found as functions of $\tilde{\tau}$ and $\tilde{\zeta}$. Let us find the integrals along the characteristics of these equations. These integrals must satisfy the equation

$$\frac{\partial \lambda_\alpha}{\partial \tilde{\zeta}} + \frac{\gamma}{\sqrt{\gamma^2 - 1}} \frac{\partial \lambda_\alpha}{\partial \tilde{\tau}} = 0 \ ; \quad \alpha = 1,2 \ \ldots . \qquad \ldots \ (2.11)$$

It is possible to find three such integrals. From (2.3) we can derive the equation

$$\frac{\partial}{\partial \tilde{\zeta}}(\gamma_0 \gamma - \sqrt{\gamma_0^2 - 1}\ \sqrt{\gamma^2 - 1}) + \frac{\gamma}{\sqrt{\gamma^2 - 1}} \frac{\partial}{\partial \tilde{\tau}} (\gamma_0 \gamma - \sqrt{\gamma_0^2 - 1}\ \sqrt{\gamma^2 - 1})$$

$$= - \gamma_0 \tilde{\varepsilon} + \frac{\gamma}{\sqrt{\gamma^2 - 1}} \sqrt{\gamma_0^2 - 1}\ \tilde{\varepsilon} \ . \qquad \ldots \ (2.12)$$

Adding equations (2.12) to (2.10) multiplied by ε, one finds the first integral

$$\lambda_1 = \frac{\tilde{\varepsilon}^2}{2} + \gamma \gamma_0 - \sqrt{\gamma_0^2 - 1}\ \sqrt{\gamma^2 - 1} \ . \qquad \ldots \ (2.13)$$

To find the next integral we notice that

$$\gamma_0 - \frac{\gamma}{\sqrt{\gamma^2 - 1}} \sqrt{\gamma_0^2 - 1} = \frac{\partial}{\partial \tilde{\zeta}} (\gamma_0 \tilde{\zeta}) - \frac{\gamma}{\sqrt{\gamma^2 - 1}} \frac{\partial}{\partial \tilde{\tau}} \sqrt{\gamma_0^2 - 1}\ \tilde{\tau}$$

$$= \frac{\partial}{\partial \tilde{\zeta}} (\gamma_0 \tilde{\zeta} - \sqrt{\gamma_0^2 - 1}\ \tilde{\tau}) + \frac{\gamma}{\sqrt{\gamma^2 - 1}} \frac{\partial}{\partial \tilde{\tau}} (\gamma_0 \tilde{\zeta} - \sqrt{\gamma_0^2 - 1}\ \tilde{\tau}) \qquad \ldots \ (2.14)$$

and thus from (2.10)

$$\lambda_2 = \tilde{\varepsilon} - \gamma_0 \tilde{\zeta} + \sqrt{\gamma_0^2 - 1}\ \tau \ . \qquad \ldots \ (2.15)$$

The third integral can be found if we use (2.13) to express ε through γ :

$$\tilde{\varepsilon} = \pm \sqrt{2} \sqrt{\lambda - \gamma_0 \gamma + \sqrt{\gamma_0^2 - 1} \sqrt{\gamma^2 - 1}} \,. \qquad \ldots (2.16)$$

Thus (2.3) can be written in the form:

$$\frac{\partial}{\partial \tilde{\zeta}} \int^{\gamma} \frac{d\gamma}{\sqrt{2\lambda - \gamma_0 \gamma + \sqrt{\gamma_0^2 - 1} \sqrt{\gamma^2 - 1}}} + \frac{\gamma}{\sqrt{\gamma^2 - 1}} \times$$

$$\frac{\partial}{\partial \tau} \int^{\gamma} \frac{d\tau}{\sqrt{2\lambda - \gamma_0 \gamma + \sqrt{\gamma_0^2 - 1} \sqrt{\gamma^2 - 1}}} = -1 = -\left(\frac{\partial}{\partial \tilde{\zeta}} + \frac{\gamma}{\sqrt{\gamma^2 - 1}} \frac{\partial}{\partial \tilde{\tau}}\right) \tilde{\zeta}$$

or

$$\lambda_3 = \pm \int_{\gamma_{min}}^{\gamma} \frac{d\gamma}{\sqrt{2} \sqrt{\lambda_1 - \gamma_0 \gamma + \sqrt{\gamma_0^2 - 1} \sqrt{\gamma^2 - 1}}} \,. \qquad \ldots (2.17)$$

These three integrals are sufficient to solve the Cauchy problem. For example, suppose that $\tilde{\varepsilon} = \tilde{\varepsilon}_0(\zeta_0)$ and $\gamma = \gamma(\tilde{\zeta}_0)$ are the given initial values of ε and γ at time $t = 0$. Then taking $t = 0$ in the three integrals $\lambda_1, \lambda_2, \lambda_3$ we find the functions $\lambda_1 = \lambda_1(\tilde{\zeta}_0)$, $\lambda_2 = \lambda_2(\tilde{\zeta}_0)$, $\lambda_3 = \lambda_3(\tilde{\zeta}_0)$. These functions are constant along the characteristics which start for each given $\tilde{\zeta}_0$, so that each value of λ_α can be matched by a value of $\tilde{\zeta}_0$. Thus, for any given $\tilde{\zeta}$ and $\tilde{\tau}$ one can find the corresponding $\tilde{\zeta}_0$ as we move along the characteristic, i.e. $\tilde{\zeta}_0 = \tilde{\zeta}_0(\tilde{\zeta}, \tilde{\tau})$. The function $\tilde{\zeta}_0(\tilde{\zeta}, \tilde{\tau})$ describes the characteristics. This means that the actual solution of the Cauchy problem is described by these three integrals in which:

$$\lambda_1 = \lambda_1(\tilde{\zeta}_0(\tilde{\zeta}, \tilde{\tau})) \,, \quad \lambda_2 = \lambda_2(\tilde{\zeta}_0(\tilde{\zeta}, \tilde{\tau})) \,, \quad \lambda_3 = \lambda_3(\tilde{\zeta}_0(\tilde{\zeta}, \tilde{\tau})) \,.$$

The functions λ_1, λ_2 and λ_3 are known and thus these three integrals form a set of three equations for the unknown quantities

$$\tilde{\varepsilon}(\tilde{\zeta},\tilde{\tau}) \ , \quad \gamma(\tilde{\zeta},\tilde{\tau}) \ , \quad \zeta_0(\tilde{\zeta},\tilde{\tau}) \ , \qquad \ldots \ (2.18)$$

which can be solved. This procedure requires numerical computation; for this purpose we normalize the integrals so that one half period of the non-linear stationary wave is equal to unity.

Before doing this we must mention first that the above integrals describe a solution of the general Cauchy problem of relativistic motion of electrons whose average charge is compensated by uniform ions (not just the specific problem of the stability of the non-linear stationary wave considered below) and, secondly, that the generalization of the results to the case when the charge is not fully compensated (which can occur for a relativistic beam because of the Budker-Bennett effect) is quite simple.

For a non-linear stationary wave, the profile in the co-ordinate system considered does not depend on τ and therefore λ_α = const. Let us choose the origin of $\tilde{\zeta}$ such that in the frame of the wave $\lambda_3 = 0$. Instead of λ_1 let us introduce

$$k^2 = \frac{2\sqrt{\lambda_1^2 - 1}}{\lambda_1 + \sqrt{\lambda_1^2 - 1}} \ . \qquad \ldots \ (2.19)$$

The value of k^2 characterises the amplitude of the non-linear wave (see below). Instead of γ_0 we introduce

$$k_0^2 = \frac{2\sqrt{\gamma_0^2 - 1}}{\gamma_0 + \sqrt{\gamma_0^2 - 1}} , \qquad \ldots (2.20)$$

where k_0^2 characterises the phase velocity of the wave.

Instead of γ we introduce θ :

$$\gamma = \tfrac{1}{2}\left(L + \frac{1}{L} \right), \qquad L = \frac{1 - k^2 \sin^2\theta}{\sqrt{(1 - k^2)(1 - k_0^2)}} . \qquad \ldots (2.21)$$

Because $\gamma > 1$ (see (2.3)) we have $L_{min} > 1$. Then L_{min} corresponds to $\sin^2\theta = 1$ and therefore

$$k^2 < k_0^2 . \qquad \ldots (2.22)$$

This is the condition for the absence of overtaking or multiple velocities in the stationary structure of a strong non-linear wave. The maximum and minimum values of γ in the wave can be found as the roots of the expression under the square root of the integral (2.17)

$$\gamma_{max} = \lambda\,\gamma_0 + \sqrt{\gamma_0^2 - 1}\,\sqrt{\lambda_1^2 - 1}$$
$$\gamma_{min} = \lambda\,\gamma_0 - \sqrt{\gamma_0^2 - 1}\,\sqrt{\lambda_1^2 - 1} \qquad \ldots (2.23)$$

and

$$\gamma_{max} - \gamma_{min} = 2\sqrt{\gamma_0^2 - 1}\,\sqrt{\lambda_1^2 - 1} \simeq 2\gamma_0^2 \quad \text{if} \quad \lambda_1 \to \gamma_0 , \quad \gamma_0 \gg 1 . \qquad \ldots (2.24)$$

This result corresponds to the above-mentioned maximum potential well (1.2). The same result follows from (2.21).

L_{max} corresponds to $\theta = 0$ and

$$\gamma_{max} \simeq \tfrac{1}{2} L_{max} \simeq \frac{1}{2\sqrt{(1 - k^2)(1 - k_0^2)}} \simeq \frac{1}{2(1 - k_0^2)} = 2\,\gamma_0^2 . \qquad \ldots (2.25)$$

The electric field $\tilde{\varepsilon}$ can easily be found from (2.13) and (2.21)

$$\tilde{\varepsilon} = \frac{k^2 \sin 2\theta}{2(1-k^2)^{\frac{1}{4}} \sqrt{1-k^2\sin^2\theta}} , \qquad \ldots (2.26)$$

and the integral (2.17) can be expressed through eliptical integral,

$$\frac{2k_o^2 E(k,\theta)}{\sqrt{2}(1-k_o^2)^{\frac{1}{2}}(1-k^2)^{\frac{1}{2}}} + \frac{k^2\sqrt{1-k_o^2}\sin 2\theta}{\sqrt{2}\sqrt{1-k^2}\sqrt{1-k^2\sin^2\theta}} = \tilde{\zeta} . \qquad (2.27)$$

where

$$E(k,\theta) = \int_0^\theta \sqrt{1-k^2\sin^2\theta_1}\, d\theta_1 . \qquad \ldots (2.28)$$

These results for the structure of the relativistic stationary wave were found by TSYTOVICH (1962). Let us denote ζ_p for the half-period of the wave

$$\zeta_p = \frac{2k_o^2 E(k)}{\sqrt{2}(1-k_o^2)^{\frac{1}{2}}(1-k^2)^{\frac{1}{4}}} \qquad \ldots (2.29)$$

where

$$E(k) = \int_0^{\pi/2} \sqrt{1-k^2\sin^2\theta_1}\, d\theta_1 \qquad \ldots (2.30)$$

is the complete eliptical integral. Let us also introduce the space and time co-ordinates ζ and τ respectively, and electric field ε, all of them normalized to the half-period value ζ_p

$$\zeta = \frac{\tilde{\zeta}}{\zeta_p} , \quad \tau = \frac{\tilde{\tau}}{\zeta_p} , \quad \varepsilon = \frac{\tilde{\varepsilon}}{\zeta_p} . \qquad \ldots (2.31)$$

Then the equation for the stationary wave has the form

$$\frac{E(k,\theta)}{E(k)} + \frac{k^2(1-k_o^2)\sin 2\theta}{2k_o^2 E(k)\sqrt{1-k^2\sin^2\theta}} = \zeta \qquad \ldots (2.32)$$

$$\varepsilon = \frac{(1 - k_0^2)\, k^2 \sin 2\theta}{E(k) \,.\, k_0^4 \,.\, \sqrt{1 - k^2 \sin^2\theta}} \qquad \ldots \ (2.33)$$

and γ is determined by equation (2.21). Equations (2.32), (2.33) and (2.21) are used in the next section to find the profile of the non-linear, large amplitude stationary wave. To solve the Cauchy problem of the wave whose initial stage is represented by a structure similar to that of the stationary non-linear wave, it is necessary to take into account these integrals. Let

$$\nu = \frac{\lambda_3}{\zeta_p} \quad \text{and} \quad \mu = \frac{\lambda_2}{\zeta_p} \,. \qquad \ldots \ (2.34)$$

Then these integrals have the form

$$\frac{E(k_1, \theta)}{E(k_1)} + \frac{k_1^2 (1 - k_0^2) \sin 2\theta}{2\, k_0^2\, E(k_1) \sqrt{1 - k_1^2 \sin^2\theta}} = \nu + \zeta \qquad \ldots \ (2.35)$$

$$\varepsilon = \frac{(1 - k_0^2)\, k_1^2 \sin 2\theta}{E(k_1) \,.\, k_0^4 \sqrt{1 - k_1^2 \sin^2\theta}} \qquad \ldots \ (2.36)$$

$$\varepsilon - \frac{2 - k_0^2}{k_0^2}\, \zeta + \tau = \mu \qquad \ldots \ (2.37)$$

where the subscript 1 indicates the new value of k from that corresponding to the stationary wave. If the perturbations are small, $\nu \ll 1$. In these integrals $k_0^2 = \text{const.}$ but not k^2. The initial perturbations can be given for ε and γ which determine λ_1 and λ_2, as well as for k^2 and ν. The later variant is more convenient for numerical computations. Thus

$$k_1^2 = k^2 + \delta k^2 \qquad \dots \ (2.38)$$

where $\delta k^2 \ll k^2$ is the perturbation. If ν and δk^2 are given, μ must be calculated by using the equations (2.35) - (2.37) for $\tau = 0$.

3. THE COMPUTATION PROCEDURE

We compute the characteristics of the integrals (2.35)-(2.37) by an iterative method, i.e. we take instead of ζ_0 some values ζ_{00} and find the corresponding values of the function

$$Q(\zeta_{00}) = \varepsilon - \frac{2 - k_0^2}{k_0^2}\zeta + \tau - \mu , \qquad \dots \ (3.1)$$

for the chosen values of the space and time co-ordinates ζ and τ respectively. By a suitable choice of the values ζ_{00} we can achieve the result that $Q(\zeta_{00}) \to 0$ and therefore that $\zeta_{00} \to \zeta_0$. The actual procedure can be divided into two stages:

(a) Determination of the integral μ by solution of the system of equations (2.35) - (2.37) for $\tau = 0$. We take $\zeta = \zeta_{00}$ and find by another iterative process the solution θ of the equation (2.35) (the functions $k_1^2(\zeta_0)$, $\nu(\zeta_0)$ chosen will be described later), substitute θ into (2.36) and calculate the value ε. From (2.37) we can then easily determine μ, taking $\tau = 0$.

(b) Solution of the system of equations (2.35) - (2.37) for given τ. We repeat the previous procedure but take for ζ and τ their true values. As a result we get one value of the function $Q(\zeta_{00})$. By a suitable iterative method we find its root ζ_0 and the corresponding values of $\varepsilon(\zeta,\tau)$ and $\gamma(\zeta,\tau)$.

Our preliminary tests showed that if multiple roots ζ_{0i} appear they are near to the first one, ζ_0, and to find them it is sufficient to explore the intervals $\langle \zeta_0 - 0.1 , \zeta_0 - 4 \times 10^{-4} \rangle$, $\langle \zeta_0 + 4 \times 10^{-4} , \zeta_0 + 0.1 \rangle$. 100 iteration steps in each interval proved in practice to be sufficient either to find them or to exclude their existence.

In our experiments we chose three different types of the functions $k_1^2(\zeta_0)$ and $\nu(\zeta_0)$, i.e. of the initial perturbations:

(a) $k_1^2(\zeta_0) = k^2$, $\nu = 0$, i.e. no perturbations at all. In this case we get the basic profile of the stationary wave (Section 4) whose time development under the influence of the fluctuations is later investigated.

(b) $k_1^2(\zeta_0) = k^2[1 + a\, s_1(\zeta_0)]$, $\nu = a\, s_2(\zeta_0)$ where a is the amplitude of the perturbation $(0.001 - 0.19)$, and $s_1(\zeta_0)$ and $s_2(\zeta_0)$ are functions which simulate the stochastic fluctuations, $|s_1|$, $|s_2| \leq 1$. Their values are generated in intervals $\Delta\zeta_0 = 1.10^{-3}$ by a semi-random generator and their intermediate values obtained by linear interpolation.

(c) $k_1(\zeta_o) = k^2[1 + a \sin(\pi p \zeta_o)]$, $\nu = a \sin(\pi p \zeta_o)$, i.e. resonant parametric fluctuations; p is the ratio of the frequencies of the perturbation and the wave (in our computations $p = 0.1, 1, 4, 10$).

To characterize the development of the wave we compute the values of the perturbations from the stationary state, i.e., $\Delta\varepsilon_i = \varepsilon_i - \varepsilon_{oi}$ and $\Delta\gamma_i = \gamma_i - \gamma_{oi}$ for $(N+1)$ values of the space co-ordinate $\zeta_i = i \cdot \Delta\zeta$, $i = 0, 1, \ldots N$, and the average values

$$\overline{\Delta\varepsilon} = \frac{1}{N+1} \sum_{o}^{N} |\Delta\varepsilon_i| , \quad \overline{\Delta\gamma} = \frac{1}{N+1} \sum_{o}^{N} |\Delta\gamma_i|$$

which we plot as functions of time (Sections 5, 7).

4. THE STRUCTURE OF STATIONARY NON-LINEAR RELATIVISTIC WAVES

It is obvious that the profiles of the stationary waves do not change in time in the absence of perturbations and it is sufficient to calculate them only for $\tau = 0$. They are shown in Fig.1 for one half periods for different values of k and k_o. It is apparent that for very different values of k and k_o the shape of ε is nearly sinusoidal and that when the value of k approaches k_o the gradient of the electric field increases in the vicinity of the point at which γ is minimum. One can expect that the instability should start to develop in this region of the wave. The maximum gradient of the electric field (see Fig.2) also indicates how far the wave is from the overtaking regime. Fig.3 shows the maximum amplitude of the wave electric field and Fig.4 the maximum value of the parameter γ which characterises the electron velocity as a function of k and k_0. The closer the phase velocity of the wave to the velocity of light ($k_0 \to 1$) the larger can be γ_{max} for a given maximum gradient of the electric field.

5. STOCHASTIC PERTURBATIONS OF THE WAVE

In this paragraph we investigate the stability properties of the waves described above, when we assume both small (0.1%) and large (~20%) stochastic perturbations of the parameters k^2 and ν at time $\tau = 0$, corresponding to initial perturbations of the wave amplitude and electron density. An example of the shape of ϵ and γ at time $\tau = 0$ is shown in Fig.5. In order to follow the wave structure in more detail we shall present only the shape of the perturbations from the stationary state, i.e. $\Delta\epsilon = \epsilon - \epsilon_0$ and $\Delta\gamma = \gamma - \gamma_0$, as functions of the space co-ordinate ζ.

Fig.6 shows the shape of typical fluctuations $\Delta\epsilon$ and $\Delta\gamma$ at three different times. We have found no indication of any strong instability for a wide range of parameters

k and k_0 $(0.99 \geq k_0 \geq 0.4,\ 0.98 \geq k \geq 0.4,\ k < k_0)$ even though certain time variations are evident.

The time variation of the average values $\overline{\Delta\varepsilon}$ and $\overline{\Delta\gamma}$ normalized to the maximum values of $\varepsilon_{o\,max}$ and $\gamma_{o\,max}$ of the stationary wave is shown in Fig.7. The values $\overline{\Delta\varepsilon(\tau)}$ and $\overline{\Delta\gamma(\tau)}$ fluctuate ($\leq 50\%$) but never exceed their respective initial values. A similar investigation performed for various amplitudes of the initial perturbation shows (Fig.8) that the general time behaviour of the perturbations is independent of the amplitude of the initial perturbation a, and also that the relative amplitude of the perturbations $\overline{\Delta\varepsilon}/a$ decreases with a increasing, that after it exceeds some critical value ($a \approx 0.02$ in our example in Fig.8) some form of saturation is observed.

We must emphasise that the small perturbations of the amplitude lead to small perturbations of the electric field in almost all regions of ζ observed except close to the place of maximum electric field gradient. The initial large perturbations of ε near to this point may make it impossible to observe the development of instability in this region. To avoid this effect we modulate the amplitudes $s_1(\zeta_0)$ and $s_2(\zeta_0)$ of the random fluctuation of k^2 and ν respectively, (i.e., decrease their amplitude near to the points $\zeta = \pm 1,\ \pm 3,\ \pm 5,\ \ldots$) so that the initial amplitude of the electric fluctuations at time $\tau = 0$ is approximately constant all along the wave. Fig.9 illustrates the time development of the fluctuations in the region of large electric field gradient. Although we have avoided the large initial perturbation in the vicinity of the high electric field gradient, large fluctuations quickly appear there. They appear as the propagation of the initially small perturbation along the ζ-coordinate away from the high field gradient region, and undamped perturbations enter this region where they are amplified; the whole effect repeats periodically. This seems to support the argument that the development of a perturbation in the region of high electric field is essentially independent of the initial perturbation in this region.

6. MULTISTREAM INSTABILITY

The development of a small perturbation can lead to a situation in which we can find two or more different values for the particle velocity at the same position and time. This indicates that there exist two plasmas penetrating one through another. As we have described above, our programme can find these two roots or preclude their existence. It enables us to determine the regions of ζ where the two roots exist, as a function of time. Figs.10a, b , c, show such time development for different parameters k and k_0.

The two roots first appear exactly in the regions of high electric field gradient but then spread into the wider region. It is interesting to note that in the case of a highly relativistic wave (Fig.10c) the region in which there are two roots is considerably smaller than in the other examples (Fig.10 a ,b).

The time τ_0 when these two roots start to appear is plotted as a function of k and k_0 in Fig.11. Note that one can find such a combination for k and k_0 that the two roots do not appear at all, (for example $k_0 = 0.99$, $k \sim 0.7$). The absence of two roots in such a condition was checked for a very long time τ (up to 40). It is also interesting to note that the larger the phase velocity of the wave (i.e. the nearer k_0 is to unity) the easier it is to find the conditions when only one root exists. Thus the larger is γ_0 (i.e. the more relativistic is the wave) the less likely is interstreaming to occur. The appearance of two roots does not necessarily mean that the overlapping is in any way dangerous and actually destroys the wave.

As the results show, the difference

$$\Delta\gamma = \gamma_1 - \gamma_2 \ll \frac{\gamma_1 + \gamma_2}{2} = \bar{\gamma} .$$

Therefore, in the frame of reference moving with the velocity $u = \sqrt{1 - \frac{1}{\bar{\gamma}^2}}$ (in which the two streams have equal and opposite velocities) the velocities of the beams are not relativistic and their absolute values are equal to

$\frac{|\Delta\gamma|}{\bar{\gamma}}$. The characteristic length for development of this instability is of the order:

$$\tilde{\zeta}_c \simeq \frac{\Delta\gamma}{\gamma} \frac{1}{\omega_{pe}} \sqrt{\frac{I}{\gamma_0}} \quad . \qquad \ldots (6.1)$$

If we divide it by ζ_p we get the dimensionless characteristic length

$$\zeta_c \simeq \frac{\Delta\gamma}{\gamma}(1 - k_0^2)^{\frac{3}{4}} (1 - k^2)^{\frac{1}{4}} \quad . \qquad \ldots (6.2)$$

If $\zeta_c < \Delta\ell$ where $\Delta\ell$ is the characteristic width of the region of two roots, the instability has sufficient time to develop. Our results show that typically $\zeta_c \approx 0.005 \div 0.1$ and therefore this situation arises very quickly. It can be imagined that a region exists in which the velocity is continuously distributed between γ_1 and γ_2 as result of development of this instability. However this does not necessarily disturb the shape of the wave since $|\gamma_1 - \gamma_2| \ll \gamma$.

7. RESONANT PARAMETRIC PERTURBATIONS

It is known that a high frequency field applied to plasma can lead to parametric instability (SILIN, 1967). Further, the stabilization of drift waves by intense high frequency fields has been described by FAINBERG and SHAPIRO (1966, 1967). In these papers an arbitrary sinusoidal non-self consistent high frequency field was considered. Notice that the plasma polarization can change the structure of an intense wave and its parametric stability. The large amplitude wave is an example of a self-consistent high frequency electric field which takes into account the plasma polarization. One interesting question is whether the parametric resonance still occurs in this case. We can analyze this problem for any (not merely linearly-small) parametric perturbations and find the non-linear saturation of the parametric instability if it does exist at all.

Fig.12 shows the time variation of the normalized average amplitude of fluctuations for the values of parametric constant p (defined in Section 3) equal 0.1, 1, 4, 10. For $p = 1, 3, 10$ the amplitude of the electric field fluctuations initially grows ($\tau \approx 0 - 1$); in this stage a rather larger amplitude is observed for larger values of p. In the following time development we can see the non-linear saturation and subsequent decay of the fluctuations. Note that these features are most pronounced for $p = 1$ closest to parametric resonance. Similarly, as in the case of the stochastic initial perturbations, the maximum fluctuations appear near to the points with maximum electric field gradients (Fig.13). A rather special situation was found in the case $p = 0.1$. The growth and non-linear saturation described above are here barely noticeable, but an interesting phenomenon (shown in Fig.14) similar to that of second sound can be observed: the perturbations form another 'wave' (see dashed envelope) which propagates along the initial wave.

We have investigated the existence of two roots for the parametric instabilities and have found that they are mostly absent, or sometimes appear in single, isolated points (but not in large areas as for stochastic initial perturbations) for large values of p $(p = 10)$ with the values of γ_1, γ_2 very near one to another and it is not excluded that their appearance is due only to computational rounding errors.

8. CONCLUSIONS

The amplitude of perturbations of the large amplitude relativistic non-linear wave vary with time to a certain extent, but none of them grows significantly. If the initial perturbations are stochastic, they are slightly damped; in the case of parametric initial perturbations a perturbation growth was found followed by a non-linear saturation and decay.

Under some conditions two different values of particle velocities γ_1, γ_2 can be found at the same position and time, indicating the development of particle interstreaming and instabilities in the wave.

The difference between the solutions γ_1, γ_2 is very small and leads only to the formation of a 'layer' on the wave in which velocities of the particles are distributed between γ_1 and γ_2. As the 'thickness' of the layer is small compared to the maximum velocity of wave particles, it does not essentially influence the large potential wells in the wave (i.e. does not destroy them). A more detailed study of the interstreaming instabilities as well as the influence of ions on the stability of the wave are beyond the scope of this paper.

ACKNOWLEDGEMENTS

The authors wish to thank Dr R.J. Bickerton and Dr S.M. Hamberger for their support and encouragement.

REFERENCES

AKHIEZER A.I. and LYUBARSKII G.Ya. (1951) DAN USSR 80, 193.

AKHIEZER A.I., LYUBARSKII G.Ya. and FAINBERG Ya.B. (1955) Uch. Zap. Khor'kovsk. Gos. Univ. 6, 73.

CRISTOFILOS N.C. (1969) Proc. Nat. Part. Acc. Conf. Wash., Lawrence Radiation Laboratory Report UCRL - 71414.

FAINBERG Ya.B. and SHAPIRO V.D. (1966) JETP Letters 4, 20.

FAINBERG Ya.B. and SHAPIRO V.D. (1967) Soviet Physics JETP 25, 189.

LASSLETT L.T. and SESSLER A.M. (1969) Proc. Nat. Part Acc. Conf. Wash. Preprint UCRL - 18589.

LINK W.T. (1967) I E E E Trans. Nucl. Sc. 14, 777.

ROWLANDS G. (1969) J. Plasma Phys. 3, 567.

RUBIN S.B. and TSYTOVICH V.N. (1964) Soviet Phys. Tech. Phys. 9, 1.

SILIN V.P. (1967) Soviet Physics JETP 24, 1242.

TSYTOVICH V.N. (1961) Soviet Physics JETP 13, 933.

TSYTOVICH V.N. (1962) Soviet Physics Doklady 7, 31.

TSYTOVICH V.N. (1970) Communications of the Joint Institute for Nucl. Res., Dubna P.9-5091.

VEKSLER V.I., SARANTSEV V.P. et al. (1967) Proc. of the Conf. on Accelerators, Cambridge (U S A).

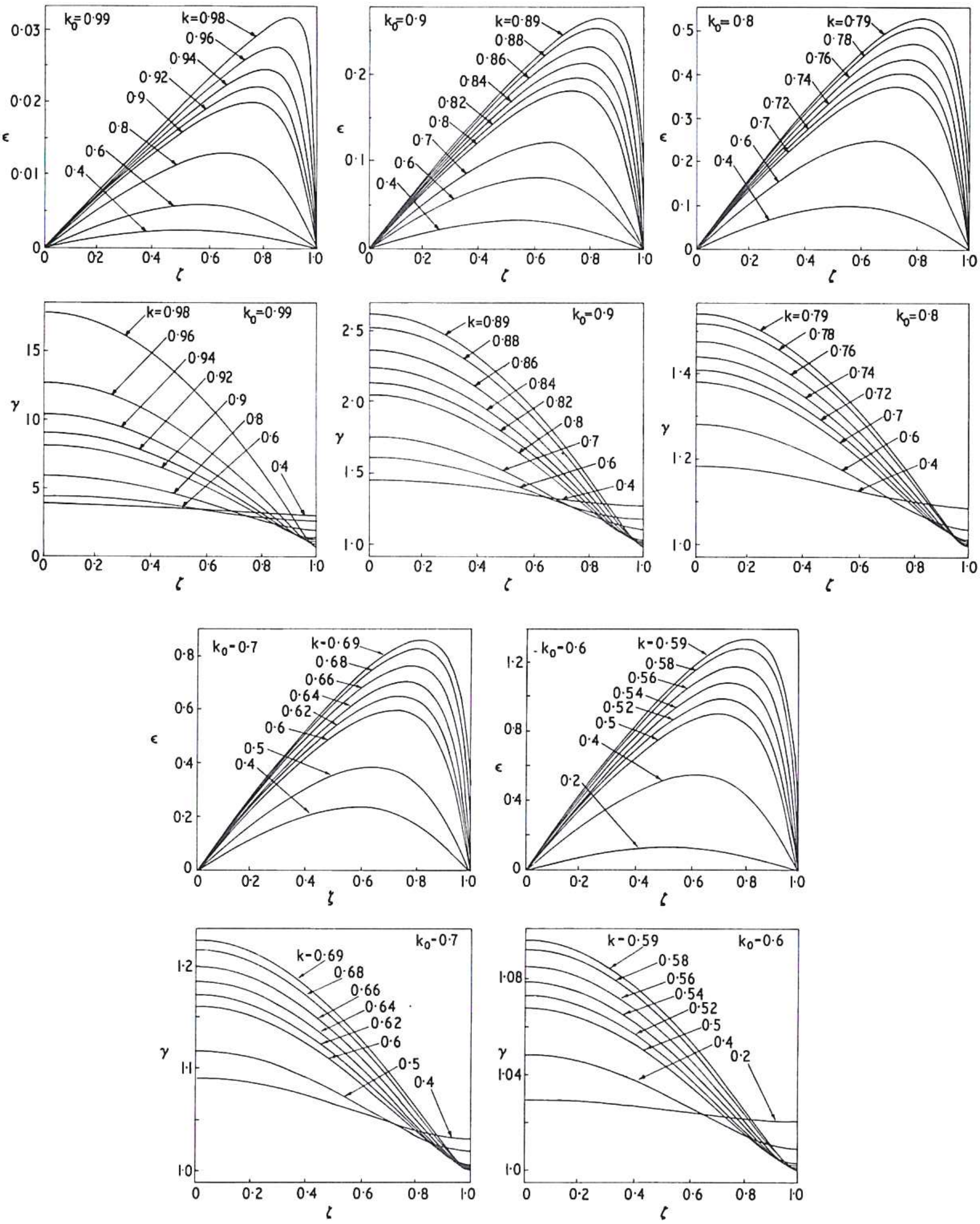

Fig.1 Shape of the stationary relativistic wave for different values of k and k_o.

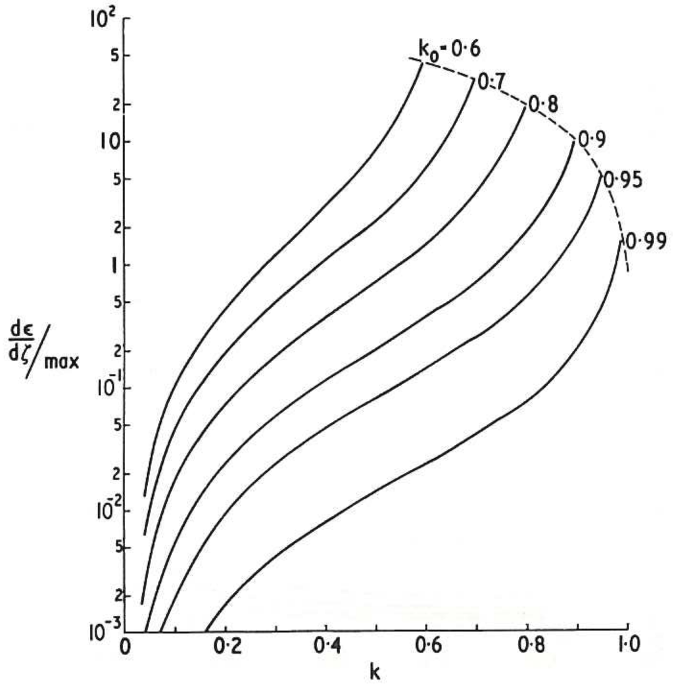

Fig.2 Maximum value of the electric field gradient of the stationary wave as function of k and k_o. The dashed line marks the onset of overtaking (Eq.2.22).

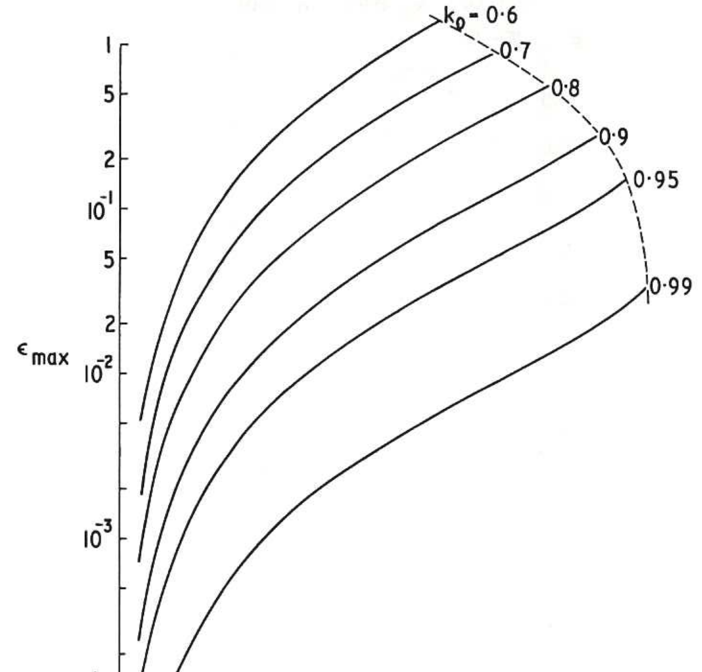

Fig.3 Maximum value of the electric field of the stationary wave as function of k and k_o. The dashed line marks the onset of overtaking (Eq.2.22).

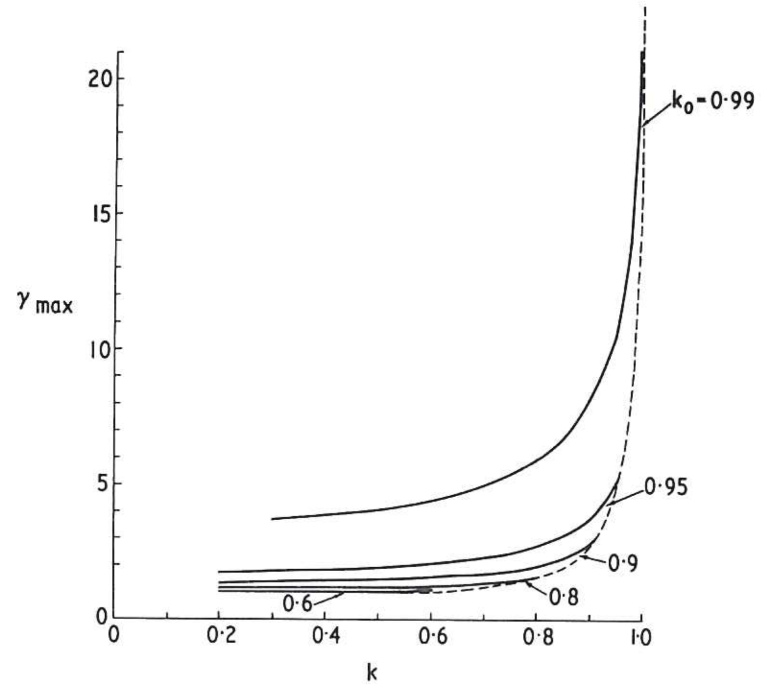

Fig.4 The maximum value of the parameter γ for the stationary wave as function of k and k_o. The dashed line marks the onset of overtaking (Eq.2.22).

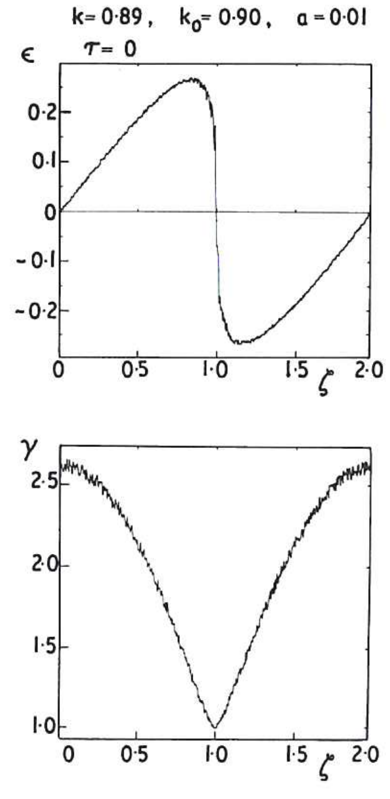

Fig.5 Example of the initial wave shape perturbed by stochastic fluctuations, N = 500.

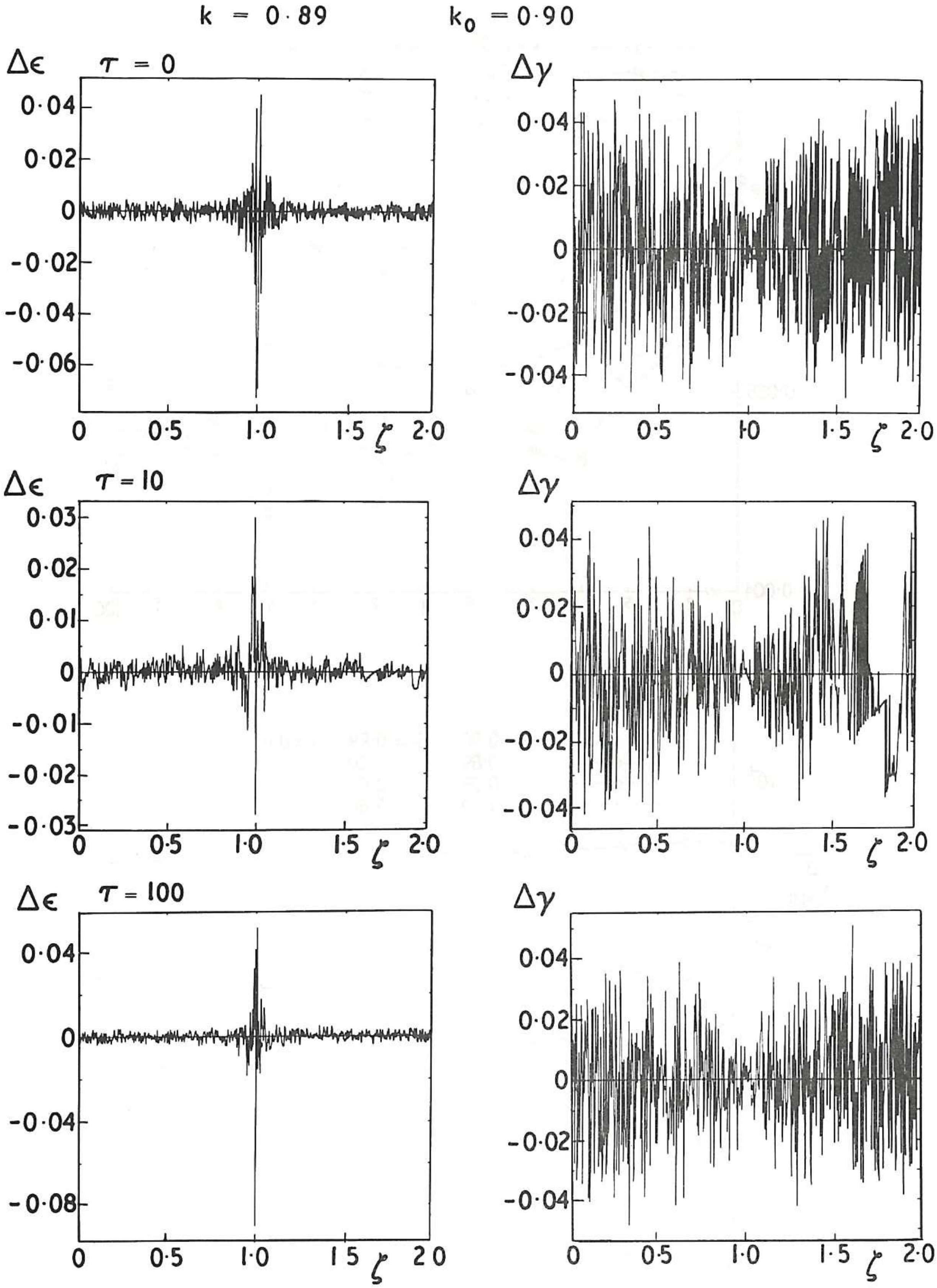

Fig.6 Example of the time development of stochastic perturbations, N = 500.

CLM-P 292

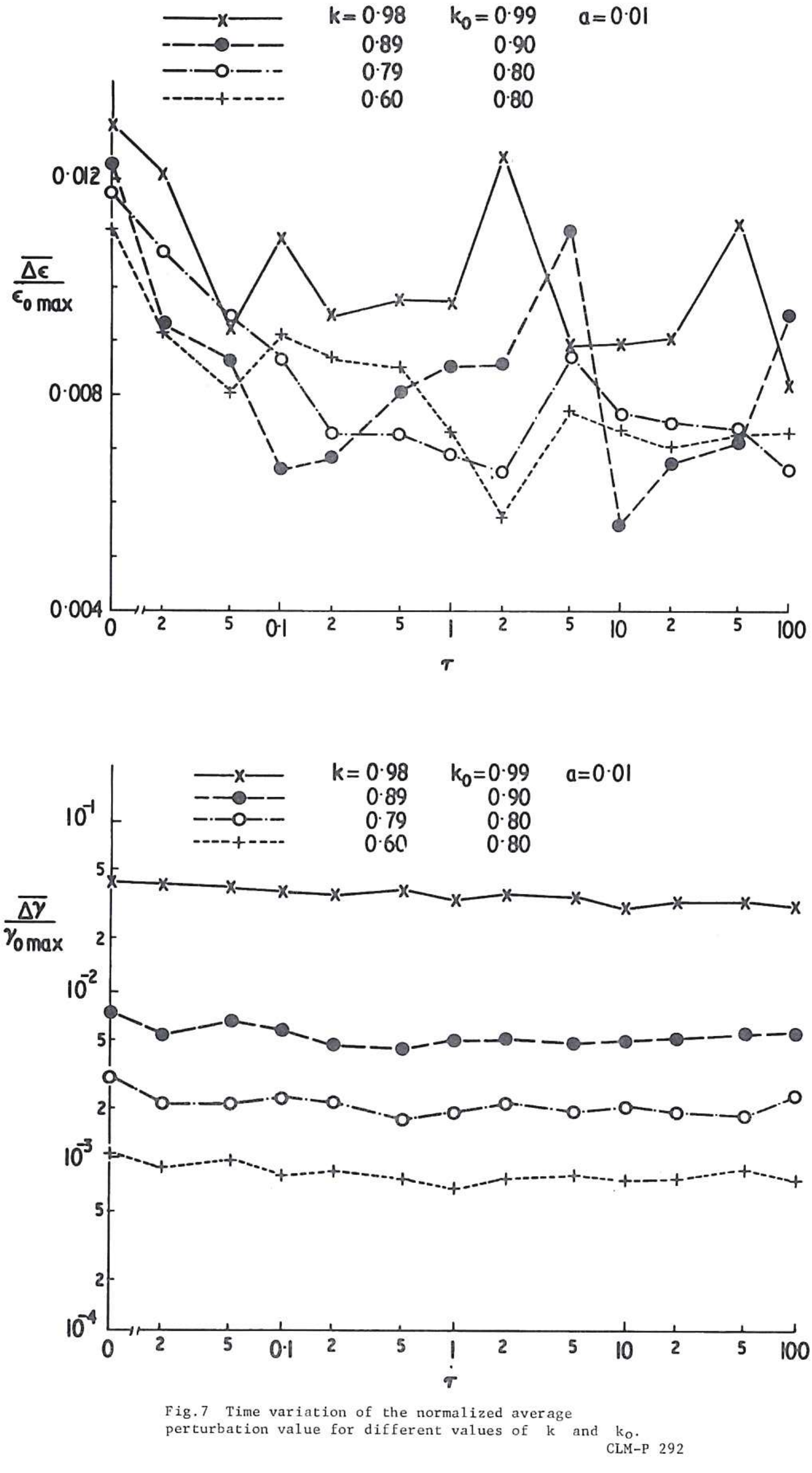

Fig.7 Time variation of the normalized average perturbation value for different values of k and k_0.

CLM-P 292

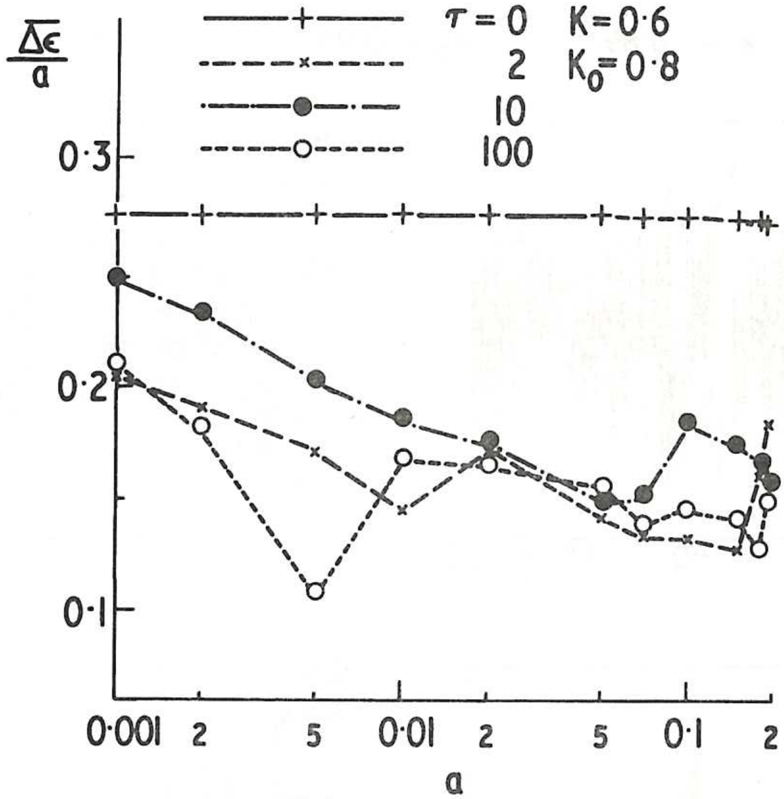

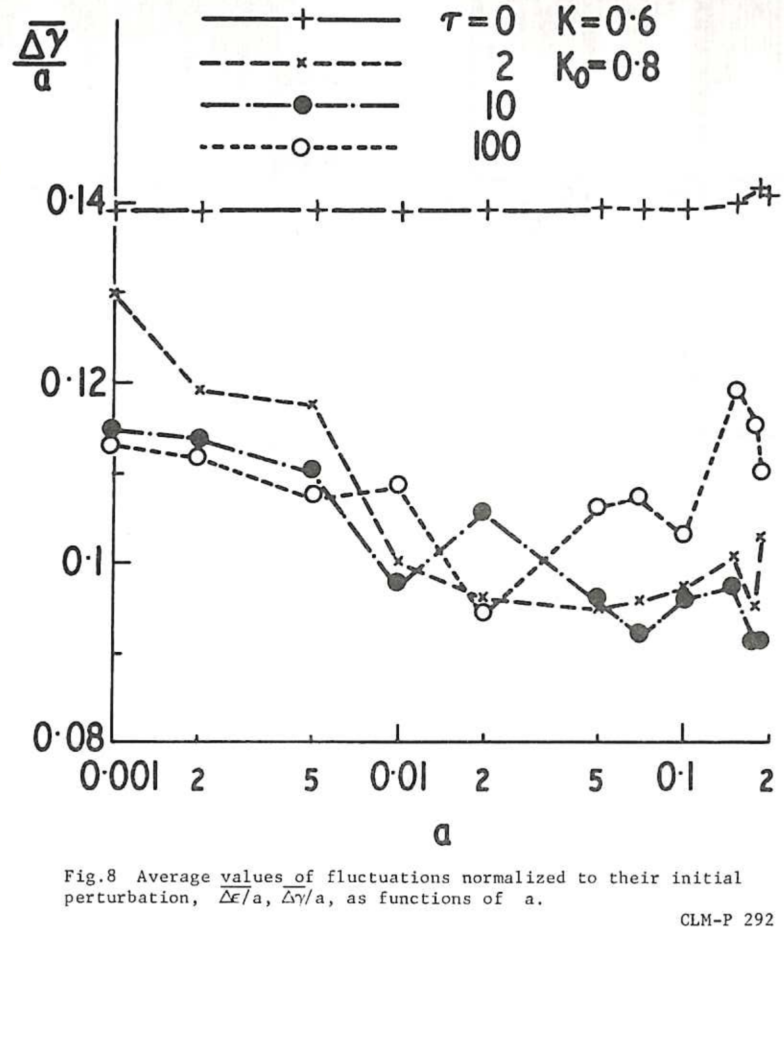

Fig.8 Average values of fluctuations normalized to their initial perturbation, $\overline{\Delta\epsilon}/a$, $\overline{\Delta\gamma}/a$, as functions of a.

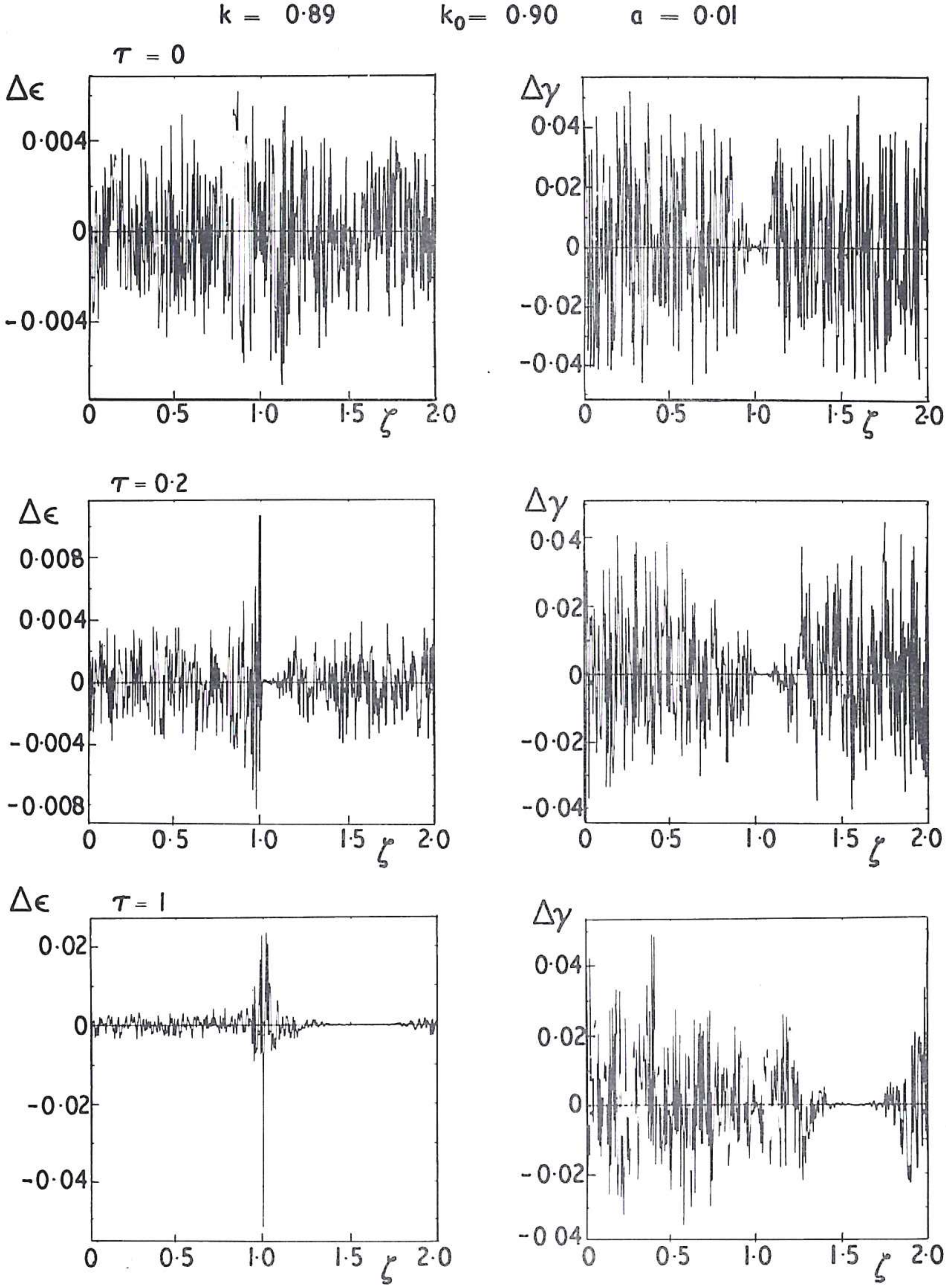

Fig.9 Time development of stochastic fluctuations with initial perturbations suppressed in the regions of high electric field gradient.

CLM-P 292

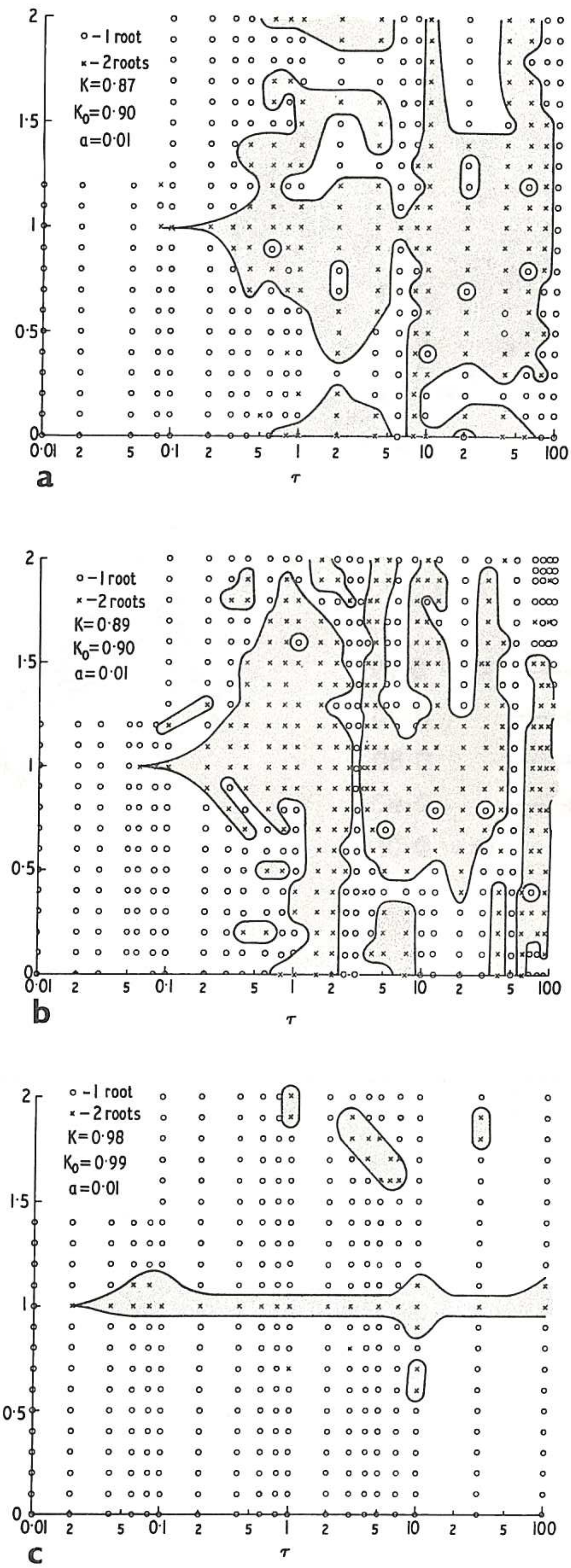

Fig.10 Region of ζ in which the particle inter-streaming appears, as a function of τ.

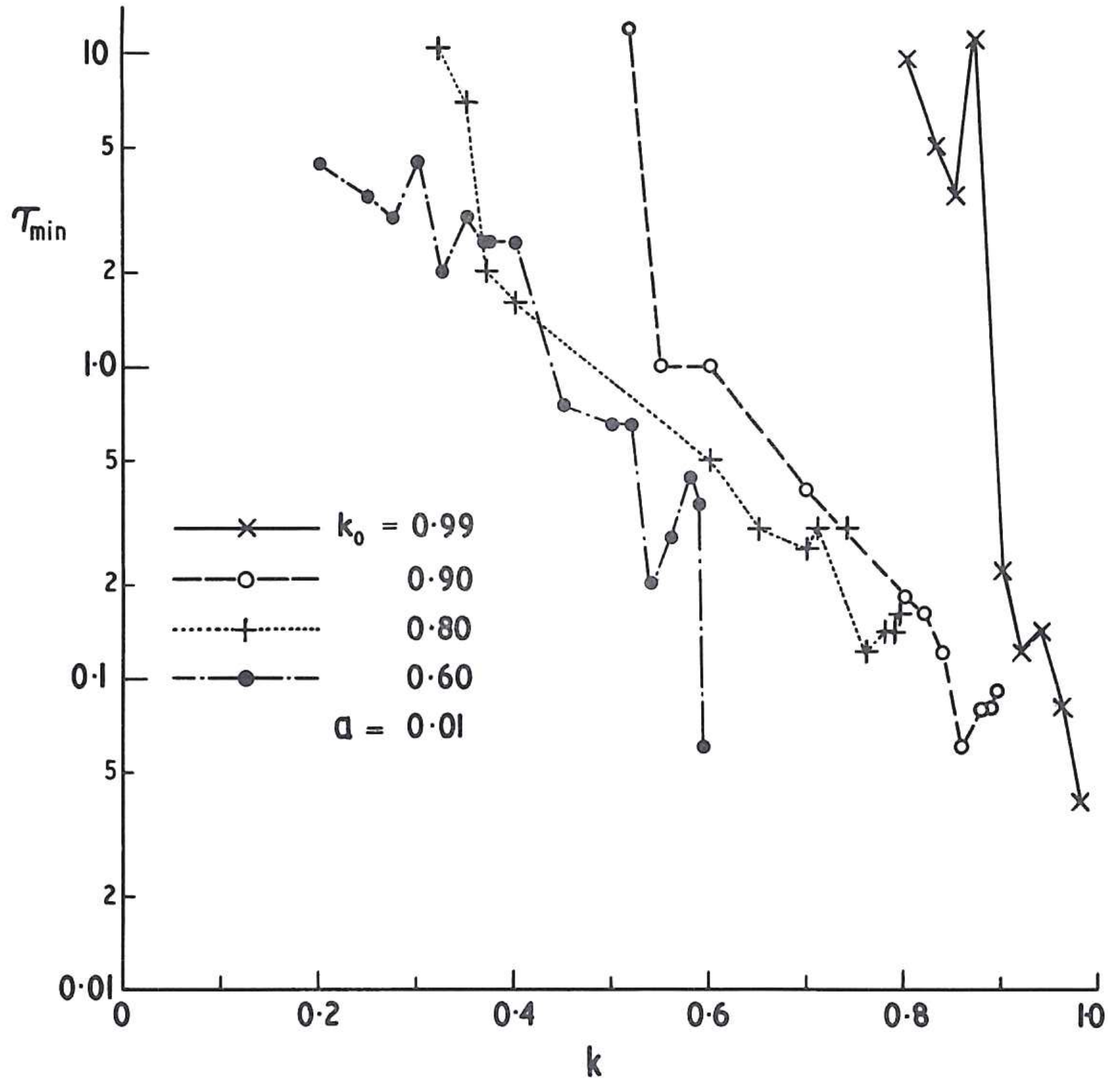

Fig.11 Time τ_o of the beginning of the appearance of inter-streaming as a function of k and k_o.

CLM-P 292

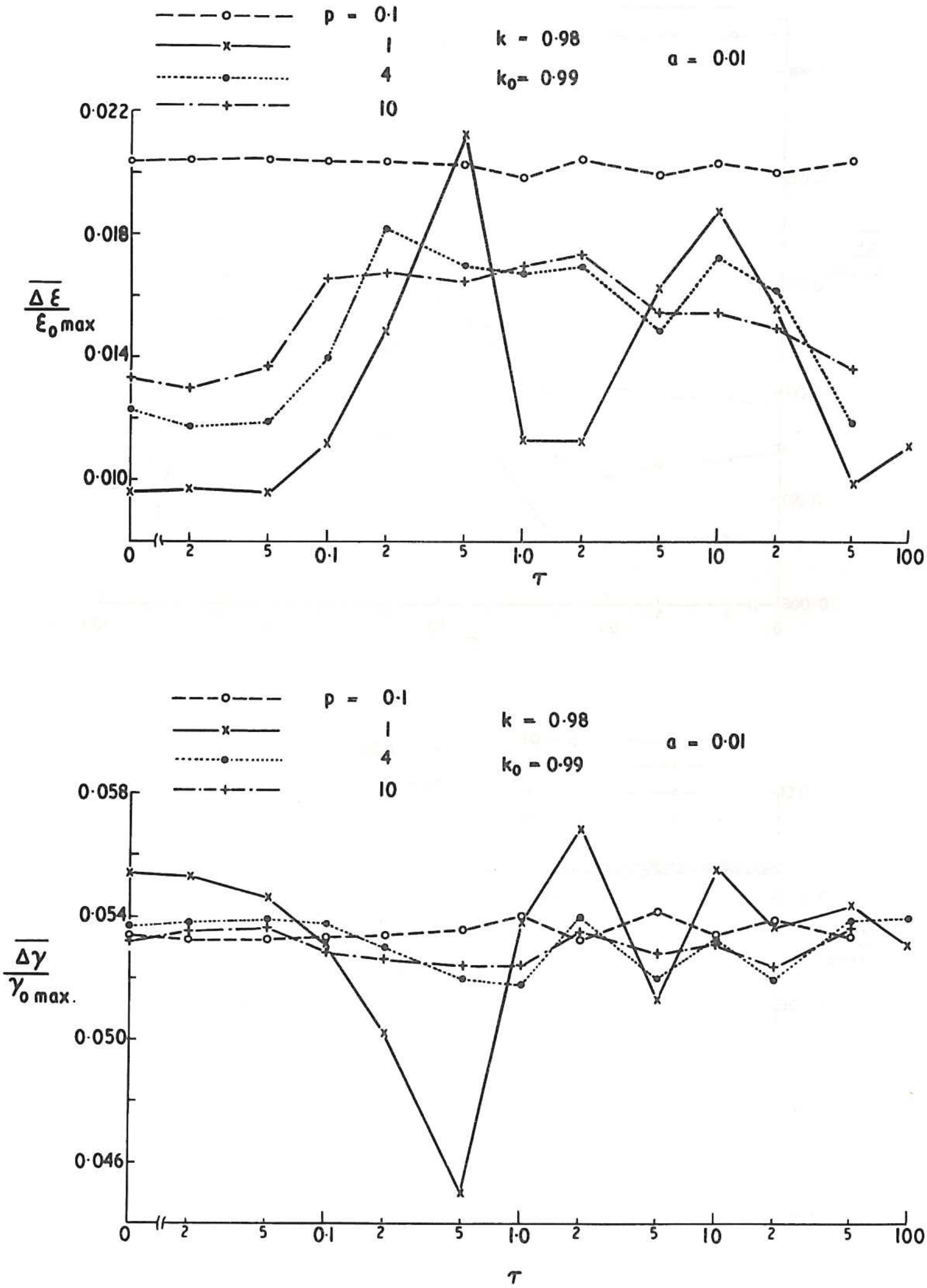

Fig.12(a) Time variation of the normalized average fluctuation value for different values of the parametric constant p.

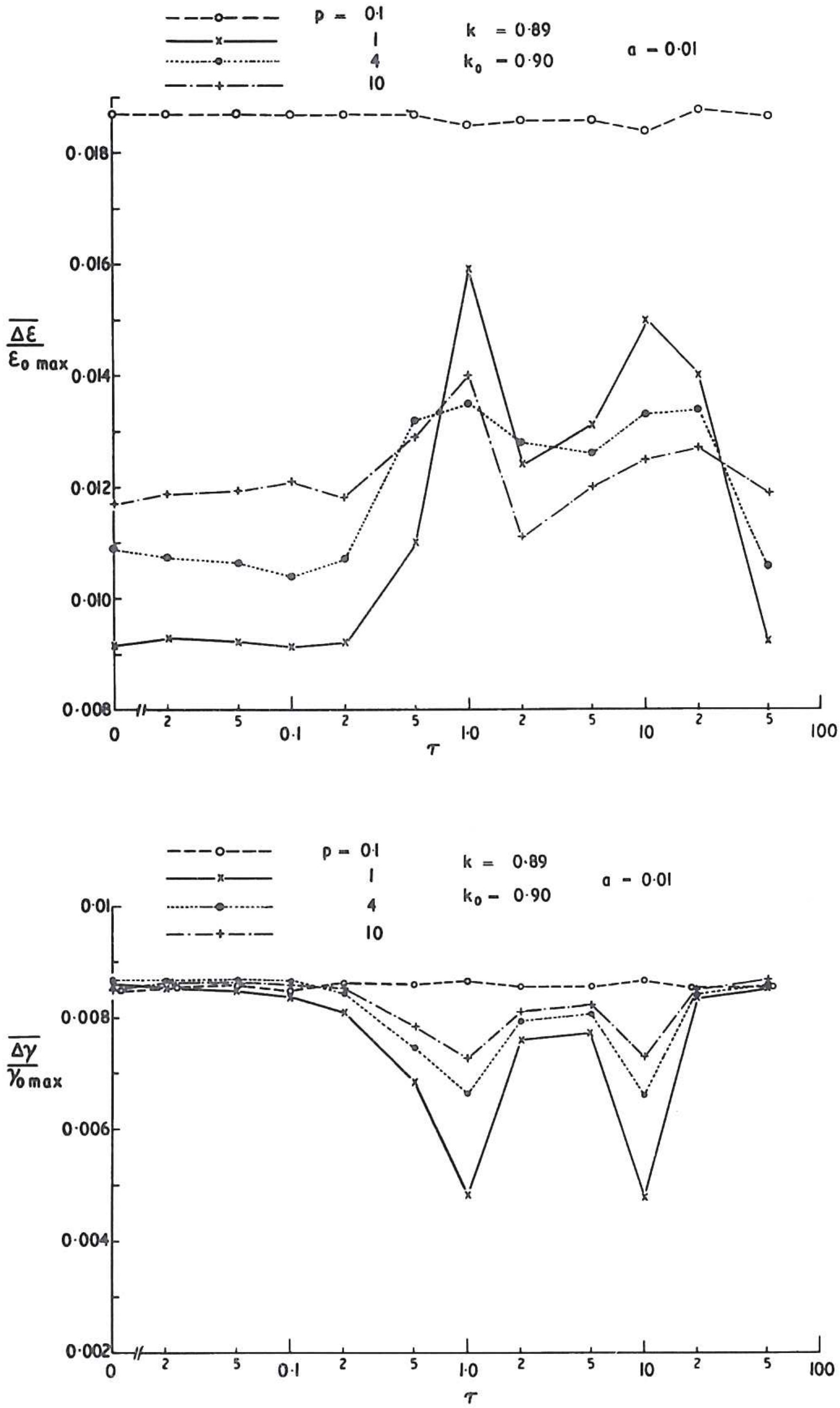

Fig.12(b) Time variation of the normalized average fluctuation value for different values of the parametric constant p.

CLM-P 292

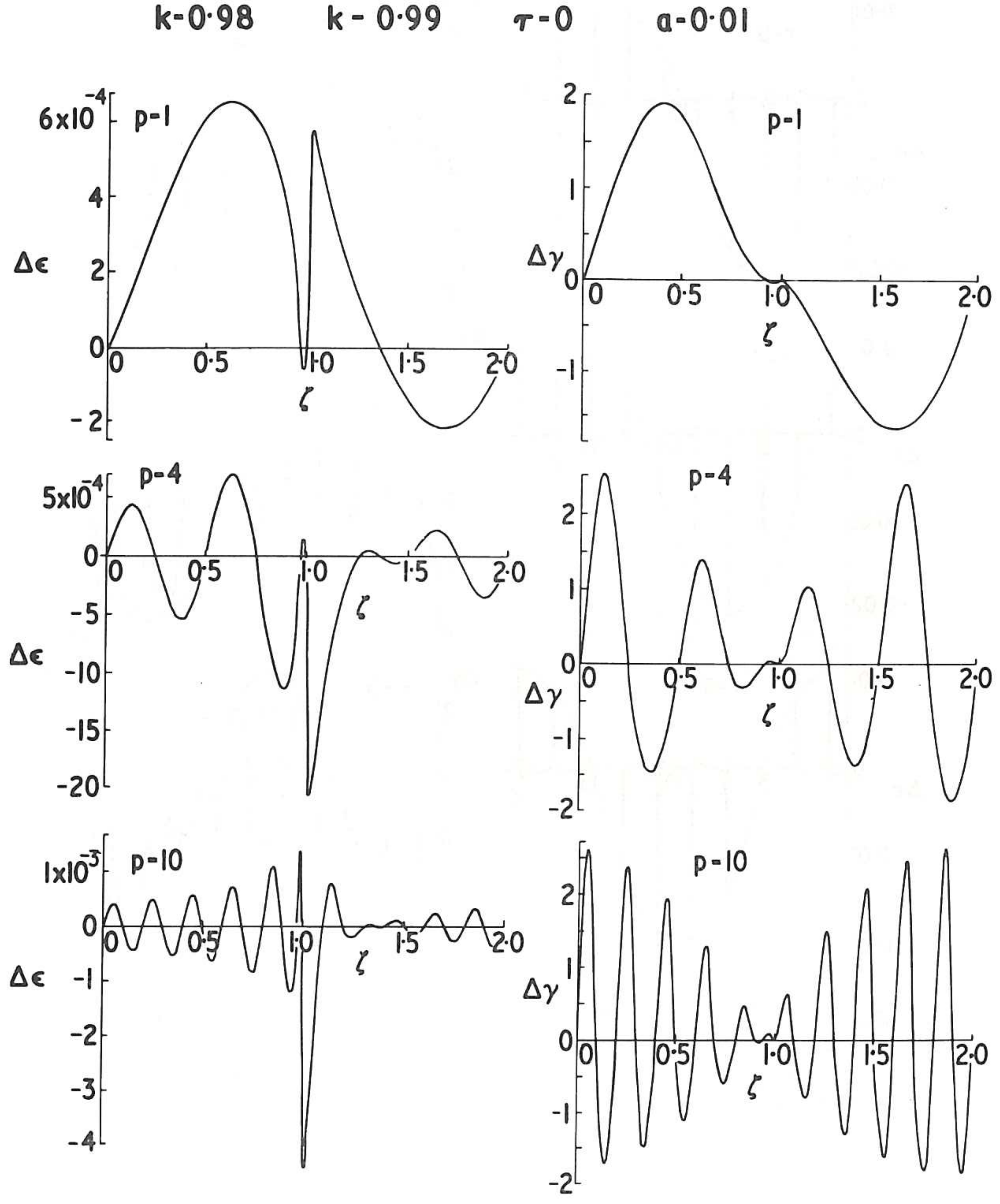

Fig.13 Shape of the initial parametric perturbations for p = 1, 3, 10.

CLM-P 292

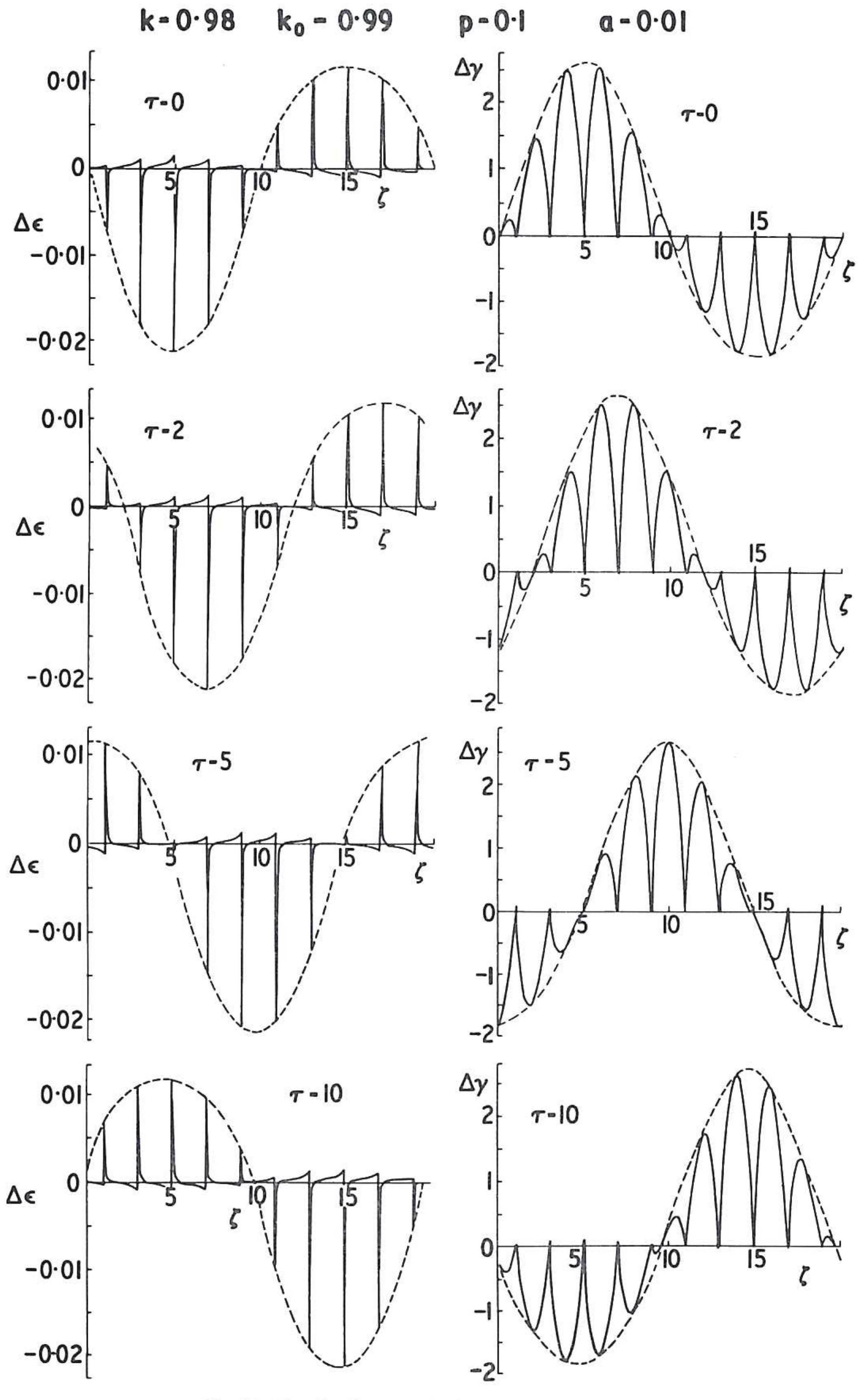

Fig.14 Time development of fluctuations for p = 0.1.
CLM-P 292